Available online at www.sciencedirect.com
SCIENCE DIRECT®
Geomorphology 54 (2003) 245–255
GEOMORPHOLOGY
www.elsevier.com/locate/geomorph

Wind velocity and sand transport on a barchan dune

G. Sauermann[a,*], J.S. Andrade Jr.[b], L.P. Maia[c], U.M.S. Costa[b], A.D. Araújo[d], H.J. Herrmann[a]

[a] *Institute for Computer Applications 1, University of Stuttgart, Pfaffenwaldring 27, D-70569 Stuttgart, Germany*
[b] *Departamento de Física, Universidade Federal do Ceará, 60455-970, Fortaleza, Brazil*
[c] *Departamento de Geologia, Universidade Federal do Ceará, 60455-970, Fortaleza, Brazil*
[d] *Universidade Estadual Vale do Acara, Sobral, Cear, Brazil*

Received 25 June 2001; received in revised form 18 June 2002; accepted 3 December 2002

Abstract

We present measurements of wind velocity and sand flux performed on the windward side of a large barchan dune in Jericoacoara, northeastern Brazil. From the measured profile, we calculate the air shear stress using an analytical approximation and treat the problem of flow separation by an heuristic model. We find that the results from this approach agree well with our field data. Moreover, using the calculated shear velocity, we predict the sand flux according to well-known equilibrium relations and with a phenomenological continuum saltation model that includes saturation transients and thus allows for nonequilibrium conditions. Based on the field data and theoretical predicted results, we indicate the principal differences between saturated and nonsaturated sand flux models. Finally, we show that the measured dune moves with invariant shape and predict its velocity from our data and calculations.

Keywords: Wind velocity; Sand transport; Barchan dune

1. Introduction

A wide variety of dune shapes can be found in deserts, on the sea-bottom, and on Mars and have been fitted into numerous classifications by geoscientists (Bagnold, 1941; Pye and Tsoar, 1990; Lancaster, 1995). The shapes depend mainly on the amount of available sand and on the change in the direction of the wind over the year. If the wind blows steadily from the same direction throughout the year and there is not enough sand to cover the entire area, dunes shaped in a crescent, called *barchans*, develop. In order to understand the shapes and movement of dunes, aeolian processes have been studied for a long time, from the entrainment of single grains to the flux of sand as a continuum quantity. One of the most important issues has been the relation between the shear velocity u_* and the saturated sand flux $q(u_*)$. The simplest flux law, which gives a cubic relation between the shear velocity and the sand flux, was introduced by Bagnold (1936). Since that time, many new flux relations have been proposed and used by different authors. For instance, one of the most widely used flux relations is the one proposed by Lettau and Lettau (1978). These sand flux relations are relevant

* Corresponding author.

0169-555X/03/$ - see front matter © 2003 Elsevier Science B.V. All rights reserved.
doi:10.1016/S0169-555X(02)00359-8

to geomorphological problems, where they are used to calculate the erosion rate from the wind shear stress in order to predict the velocity of a dune and the evolution of a free sand surface. However, all of these flux relations assume that the sand flux is everywhere saturated. This condition is hardly fulfilled at the windward foot of an isolated dune (Weng et al., 1991), e.g., a barchan, where the bed changes rapidly from bedrock or vegetation to sand. Besides the particular conditions at the dune's foot, the sand flux may never reach saturation (Lancaster et al., 1996) on the entire windward side, where the shear velocity increases gradually from the foot to the crest. Wind tunnel measurements indicate that the typical time to reach saturation in saltation is approximately 2 s (Butterfield, 1993), which corresponds to a saturation length of the order of 10 m. This length is of the order of the dune size and cannot be neglected if the sand flux on the entire windward side is significant. Furthermore, it has been observed that the time to reach saturation increases for shear velocities close to the threshold (Butterfield, 1993). In this situation, the sand flux may never reach saturation on the entire windward side and should increase exponentially with distance from the dune's foot (Lancaster et al., 1996). In recent years, several models to calculate the wind field have been developed, from analytic boundary layer approximations to numerical solutions of the Navier–Stokes equation with an enormous computational effort. Although some previous studies have discussed the limits of the saturation approximation in detail (Weng et al., 1991), much less effort has been

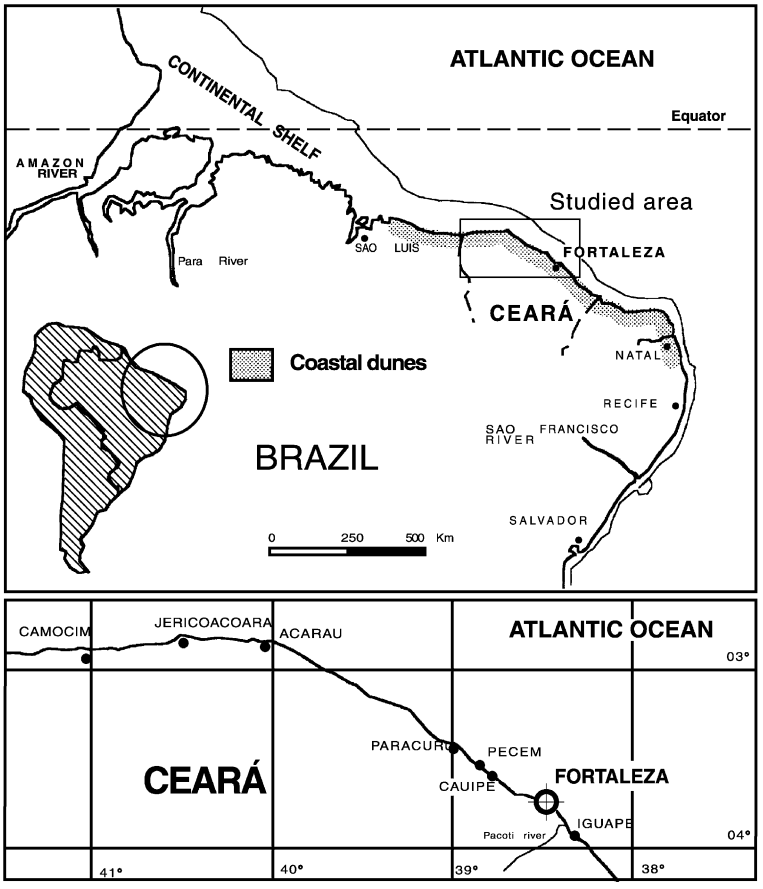

Fig. 1. Map of the study area. The dune field is located near the beach of Jericoacoara, approximately 300 km NW of Fortaleza (from Jimenez et al., 1999).

dedicated to the development of sand flux relations that effectively incorporate nonsaturation effects (van Dijk et al., 1999).

In the present work, we compare a recent phenomenological model (Sauermann et al., 2001) that allows for a nonsaturated sand flux and standard relations (Lettau and Lettau, 1978; Sørensen, 1991) with measurements performed on the windward side of a large barchan dune in Brazil, Jericoacoara. In addition, we indicate the main differences between saturated and nonsaturated sand flux models and discuss the shape-invariant movement of dunes.

2. Study area

The state of Ceará is located in northeastern Brazil (see Fig. 1). Its coastal zone is approximately 572 km long and consists mainly of long sandy beaches, interrupted only by small river mouths and rocky headlands. Almost the entire Ceará coast is backed by extensive dune fields. Three to four dune generations have been identified, but it is difficult to establish whether these were formed in one or more episodes. The last dune generation is placed on a composition of aeolianites with a cement geometry varying between isopachous and meniscus types. This generation comprises the currently active dunes, which extend along a stretch of about 6 km width along the coastline. Among them are barchans, barchanoids and sand sheets, with the dominant form depending on the available sand stock. An aerial photograph of a barchan dune field near the beach of Jericoacoara is depicted in Fig. 2. At present, the active dunes are detached from the Eastern coast by a strip of 600–2000 m wide, and are migrating on top of the older dune generations. This field has been studied before by Jimenez et al. (1999). Maia (1998) estimated that the original conditions for the dune formation were given in a period of low sea level during the last 2000 years.

3. Regional climate

The regional climate of northeastern Brazil is governed by the intertropical convergence zone (ITCZ). The ITCZ is a convergence region for north-

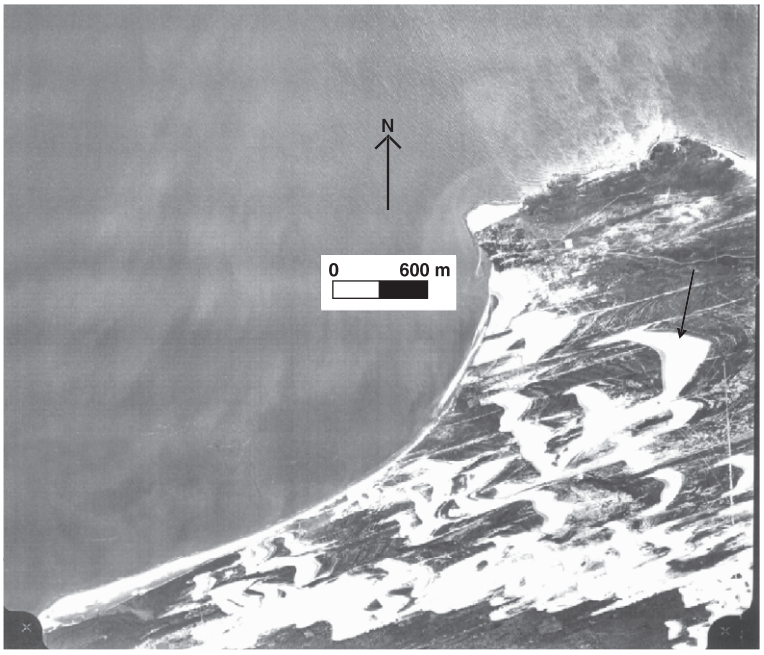

Fig. 2. Aerial photography of the dune field taken 1988 near Jericoacoara. The arrow shows the dune studied in this paper (from Jimenez et al., 1999).

easterly and southeasterly Atlantic trade winds and is characterized by an intense cloud presence and the quasi-permanent action of low atmospheric pressure centers. Seasonal latitudinal positioning of the ITCZ determines both the presence of the dominant winds and the rainfall regime (Philander and Pacanowski, 1986). Thus, when the ITCZ is located in its northernmost position, as is usually the case from August to September, intense southeasterly winds and low rainfall dominate in the area. Conversely, when the ITCZ is in its southernmost position, i.e., from March to April, weak southeasterly winds and high rainfall prevail.

Fig. 3 shows monthly rainfall statistics obtained from records for a 22-year period (1974–1995) at a meteorological station in the city of Fortaleza (see Fig. 1), which, if averaged, gives an annual rainfall of 1663 mm. However, the rainfall regime is strongly seasonal, with a wet period from January to July in which almost the entire annual rainfall is concentrated with an average yearly cumulative contribution of 1540 mm (93% of the total rainfall), and a dry period from August to December when virtually no rain falls, with an average yearly cumulative contribution of 123 mm (7% of the total rainfall). Additionally, a large inter-annual variability can also be observed, which is indicated by the maximal and minimal monthly values. This inter-annual variation, giving droughts and floods, is associated with large-scale climatological phenomena, mainly the El Niño Southern Oscillation (ENSO). This process alters the "normal" latitudinal displacement of the ITCZ, resulting in earlier northward movement during El Niño years, although the interaction mechanism has not yet been explained satisfactorily (Markham and Mclain, 1977; Hastenrath and Greischar, 1993; Nobre and Shukla, 1996).

The monthly distribution of the wind intensity obtained from data recorded over a period of 4 years (from 1993 to 1996) at the Fortaleza coast is shown in Fig. 3. The wind regime is strongly seasonal, with lower wind velocities prevailing during the wet season (average velocity of 5.47 m s^{-1}), whereas higher wind velocities occur during the dry season (average velocities of 7.75 m s^{-1}). As shown in Fig. 3, the wind direction does not show a clear seasonal pattern in the region, blowing from the east for most of the year. Throughout the year, there is a frequent southern component, especially during the dry season (from August to December). Finally, most aeolian activity is during the dry season from August to December,

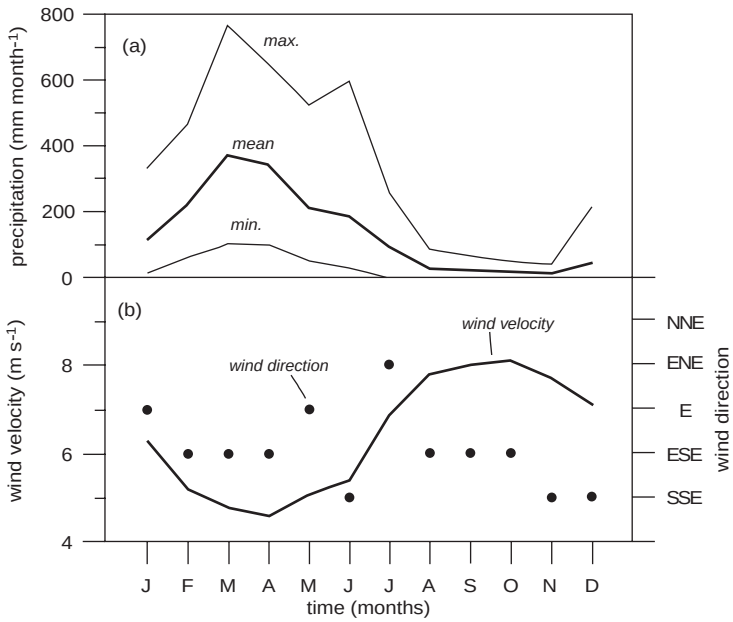

Fig. 3. (a) Rainfall throughout the year. (b) Wind direction and velocity over the year (from Jimenez et al., 1999).

where the highest wind velocities occur and the ground is dry most of the time. More details on the climate can be found in Jimenez et al. (1999).

4. Measurements

Correlated measurements of the wind velocity v and the sand flux q were performed on a large barchan dune near the beach of Jericoacoara (see Fig. 2) during the first week of December 2000, at the end of the dry season. The dune is approximately 34 m in height, 600 m in width and the length of its windward side is 200 m. A contour plot of the studied dune is depicted in Fig. 4. We obtained the height profile $h(x)$ of the windward central slice of the dune (dark line in Fig. 4) by measuring the change in height every 12 m from the top to the windward toe.

When a fully turbulent atmospheric boundary layer develops over a flat surface, it gives rise to a logarithmic velocity profile $v(z)$,

$$v(z) = \frac{u_*}{\kappa} \ln \frac{z}{z_0}, \tag{1}$$

where u_* denotes the shear velocity, z_0 the roughness length of the surface and $\kappa = 0.4$ the von Kármán constant. The shear velocity u_* has the dimensions of velocity but is defined in terms of the shear stress $\tau = \rho_{\text{air}} u_*^2$ and density ρ_{air} of the air. According to Hunt et al. (1988), the height l of the shear stress layer of wind blowing over a hill (dune) can be obtained implicitly through

$$l = \frac{2\kappa^2 L}{\ln l/z_0}, \tag{2}$$

where L is the characteristic length of the dune which is measured from the half height of the windward side to the crest, according to the definition of Hunt et al. (1988). Within the shear stress layer, velocity profiles can also be very complex as measured by Wiggs et al. (1996) on barchan dunes so that the validity of our approach is not completely settled. From Eq. (2), we obtain for $L = 100$ m and a roughness length $z_0 = 10^{-4}$ m a height of this layer of $l \approx 3.2$ m ($l \approx 4$ m for $z_0 = 10^{-3}$ m). Hence, we placed anemometers at a height of 1 m that is well inside the shear stress layer. One should note that it is very difficult to measure the wind velocity with standard anemometers within this layer for small dunes. This is the main reason for choosing such a large dune. A reference anemometer was placed approximately 300 m upwind of the dune's foot and was kept there during all the measurements. A second anemometer was placed on one point at the foot of the dune for 10 min and the average velocity was recorded. Then, the anemometer was moved 24 m uphill to the next point for 10 min. Consecutive points every 24 m were chosen until the top of the dune was reached. Finally, we normalized the average velocity $\langle v_i \rangle$ by the average velocity in the

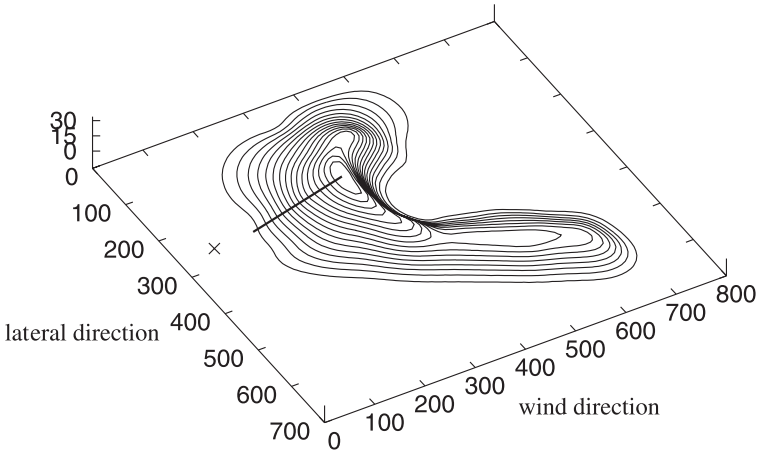

Fig. 4. Topography of the barchan dune for which our flux and velocity measurements along the central slice (shown as a dark line) have been performed. All scales are in meters. The cross shows the position of the reference station.

same period obtained from the reference anemometer, $\langle v_{r,i} \rangle$. By doing so, we could get rid of long term (≥ 10 min) variations in the wind speed time series throughout the day and obtain the shear velocity $u_{*,i}$ through

$$1 + \hat{u}_{*,i} = \frac{u_{*,i}}{u_{*0}} = \frac{\langle v_i \rangle}{\langle v_{r,i} \rangle}, \quad (3)$$

where $\hat{u}_{*,i}$ is the dimensionless shear velocity perturbation of the air caused by the dune and u_{*0} is the undisturbed shear velocity far upwind of the dune. u_{*0} can be calculated assuming a typical logarithmic profile from turbulent flow Eq. (1). During our measurements, the wind was blowing quite constantly and had an average value of 7.5 m s^{-1} at the reference station. Assuming a roughness length $z_0 = 2.5 \times 10^{-4}$ m, we obtain from Eq. (1) the undisturbed shear velocity over the plane $u_{*0} = 0.36$ m s^{-1}. The averaged and normalized measured shear velocities are plotted in Fig. 6.

Finally, we measured the sand flux on the central slice of the dune using traps consisting of a cylinder (diameter 5 cm, height 1 m) closed on the bottom and having a vertical slot of 1 cm width. It is turned with its slit facing the wind and then its bottom buried in the sand (see Fig. 5). The back-side of the traps have an opening of 2 cm covered by a fabric with pores smaller than the grain diameter. The traps were placed every 24 m from the top to the bottom of the dune, at the same positions where the wind speed was measured. Initially, they were left with their back-side in the wind direction. Then, the traps were simultaneously turned to permit the alignment of their openings with the wind direction and sand was collected during the following 15 min. From the mass m of the collected sand, the collection time T and the width w of the opening, we calculated the sand flux $q = m/(Tw)$. The measured sand fluxes are shown in Figs. 7 and 8.

5. Wind speed and shear velocity

A perturbation of the topography $h(x)$ such as a dune or a hill induces a non-local response $\hat{\tau}(x)$ on the undisturbed air shear stress τ_0 of the form,

$$\tau(x) = \tau_0[1 + \hat{\tau}(x)]. \quad (4)$$

The spatial variation of the air shear stress perturbation is crucial for understanding the stability of dunes and for predicting the sand flux onto the windward side of a dune. In a previous study (Kroy et al., 2002), we introduced a minimal model that captures the crucial features of the dynamics of sand dunes. To achieve

Fig. 5. Measuring sand flux using the depicted traps on a 35-m high barchan dune near Jericoacoara, Brazil, during the Winter 2000.

this, we used the well-known analytical approximation for flow over a gentle hill (Jackson and Hunt, 1975; Hunt et al., 1988; Weng et al., 1991) which, after some further approximations (Kroy et al., 2002), gives the following expression for the air shear stress perturbation:

$$\hat{\tau}(x) = A\left(\frac{1}{\pi}\int_{-\infty}^{\infty}\frac{h'}{x-\xi}\mathrm{d}\xi + Bh'\right), \qquad (5)$$

where h' denotes the spatial derivative of the dune's profile $h(x)$ in the wind direction. The coefficients $A(L/z_0)$ and $B(L/z_0)$ depend only logarithmically on the ratio between the characteristic length L of the dune and the roughness length z_0 of the surface. For a dune with a length and width ratio $W/L \approx 1$ and $L/z_0 = 4.0 \times 10^5$, respectively, we obtain $A \approx 3.2$ and $B \approx 0.3$. However, a value of $B \approx 0.4$ provides a much better fit to the data and suggests a roughness length greater than the assumed value of $z_0 = 2.5 \times 10^{-4}$. One should note that the shear stress calculated according to Eq. (5) is scale invariant and leads to the same speed-up n ($n = \max(\tau)/\tau_0$) for small and large dunes. This is expected in the fully turbulent regime where no characteristic length exists. Moreover, the shear stress perturbation $\hat{\tau}(x)$ given by Eq. (5), scales with the height H and inversely with the characteristic length L of the dune so that $\hat{\tau} \propto H/L$.

Eq. (5) is based on a perturbation theory and can only be applied to smooth hills. Jackson and Hunt (1975) assumed $H/L < 0.05$, whereas Carruthers and Hunt (1990) showed that for mean slopes up to $H/L \approx 0.3$, Eq. (5) gives reasonable results. The windward side of a barchan dune is always below the latter value and the formula should be applicable. However, flow separation certainly occurs at the brink of the dune and this is out of the scope of linear perturbation theory. To solve this problem, a heuristic approach has been suggested by Zeman and Jensen (1988). They introduced a separation bubble that comprises the recirculating flow (the large eddy in the wake of the dune) and extends from the brink of the dune (where the detachment takes place) to the point of reattachment. In short, the separating streamline $s(x)$ (i.e., the upper bound of the separation bubble) is defined here in terms of a third-order polynomial that is simply a smooth continuation of the profile $h(x)$ at the brink x_{brink} and at the reattachment point $x_{\mathrm{brink}} + L_{\mathrm{r}}$. In other words, we use $h(x_{\mathrm{brink}}) = s(0)$, $h'(x_{\mathrm{brink}}) = s'(0)$, $s(L_{\mathrm{r}}) = 0$ and $s'(L_{\mathrm{r}}) = 0$, where $L_{\mathrm{r}} \approx 6H$ is the downwind distance of the reattachment point from the brink. Finally, the shear stress

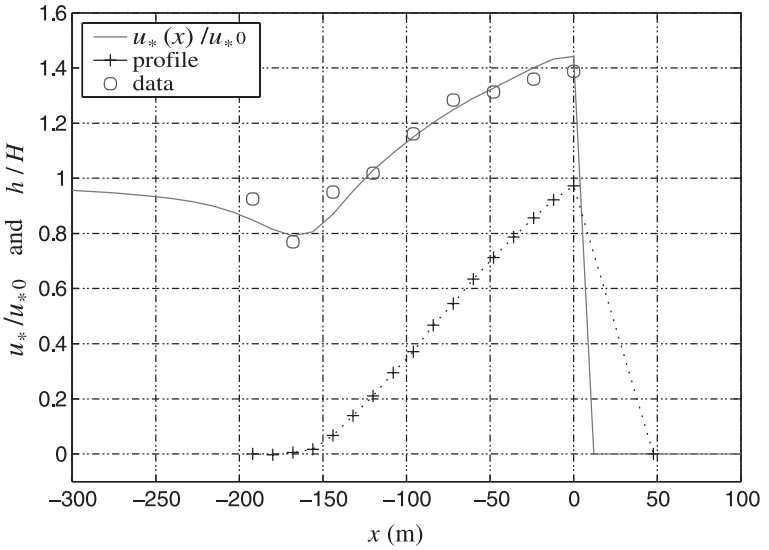

Fig. 6. The circles show the measured shear velocity u_* and wind speed v ($z = 1$ m) normalized by their reference values u_{*0} and v_0 ($z = 1$ m), respectively. The solid line depicts the prediction of Eq. (5) using the measured height profile $h(x)$ shown in the bottom curve (crosses). The depression at the dune's foot is about 0.8 and the maximum speed-up at the brink is approximately 1.4. The wind goes from left to right.

perturbation $\hat{\tau}(x)$ for the windward side of the dune is calculated using Eq. (5), the profile $h(x)$ on the windward side, and the separating streamline $s(x)$ on the lee side. The result is shown in Fig. 6 together with the measured mean values (averages over 10-min intervals) normalized according to Eq. (3). The agreement between model results and measurements is good. From this, we can conclude that the heuristic model of the separation bubble combined with the analytic expression, Eq. (5), provide a reasonable approximation for the wind field above the dune. This strategy enormously reduces the computational effort, compared to the numerical solution of turbulence models and the averaged three-dimensional Navier–Stokes equation.

6. Sand flux

In the preceding section, we have introduced a model to compute the shear velocity $u_*(x)$ and, therefore, the stationary shear stress, $\tau(x) = \rho_{\mathrm{air}} u_*(x)$, from the height profile $h(x)$. Here, we will make use of well-established phenomenological relations to determine the sand flux q from the shear velocity. For instance, the sand flux relations proposed by Lettau and Lettau (1978),

$$q_{\mathrm{L}}(u_*) = C_{\mathrm{L}} \frac{\rho_{\mathrm{air}}}{g} u_*^2 (u_* - u_{*\mathrm{t}}), \tag{6}$$

and (Sørensen, 1991)

$$q_{\mathrm{S}}(u_*) = C_{\mathrm{S}} \frac{\rho_{\mathrm{air}}}{g} u_* (u_* - u_{*\mathrm{t}})(u_* + 7.6 u_{*\mathrm{t}} + 2.05\ \mathrm{m\ s^{-1}}), \tag{7}$$

have been applied by many workers to estimate sand flux under saturated conditions. In Eqs. (8) and (9), the parameters $C_{\mathrm{L}} = 4.1$ and $C_{\mathrm{S}} = 0.48$ have been obtained by fitting these relations to wind tunnel data by White and Mounla (1991), g denotes the gravitational acceleration and $u_{*\mathrm{t}} = 0.28\ \mathrm{m\ s^{-1}}$ is the threshold for sand transport, below which the flux is zero. In Fig. 7, we show the predictions of Eqs. (6) and (7) together with the measured data. The relation (7) fits the data very well, whereas the relation by Lettau and Lettau (1978) provides a good fit only for the fluxes away from the bottom and the top of the dune. This is in accord with the calibration made in Sauermann et

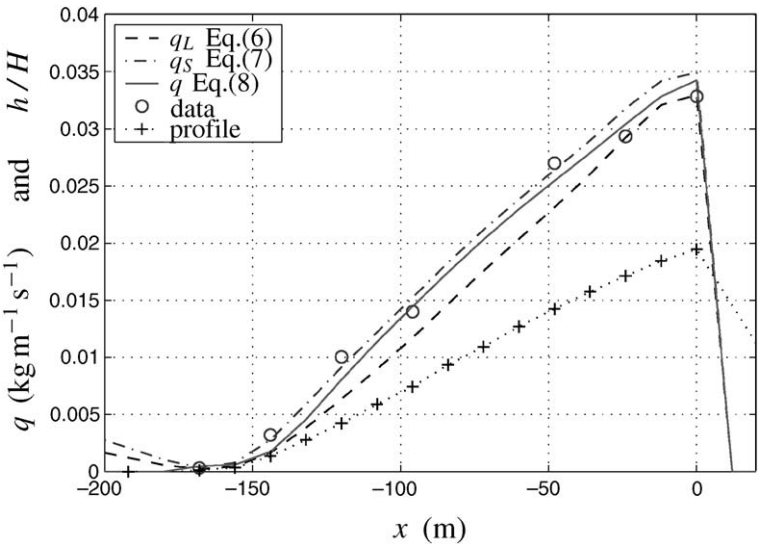

Fig. 7. Measured and calculated sand flux along the central slice of the barchan dune. The circles denote measurements, and the solid line, the prediction of the nonequilibrium sand flux model, Eq. (8). The saturated sand flux obtained by Eqs. (6) and (7) is also depicted. However, these saturated sand flux relations cannot correctly predict the sand flux near the dune's foot and show clearly that the assumption of saturation breaks down. The wind goes from left to right.

al. (2001), where relation (7) reproduced well the structure of the wind channel data in contrast to relation (6).

If a sand flux relation of the type $q(u_*)$ is applied, we have to keep in mind that this implies that the saltation process is in equilibrium, and therefore, the sand flux should be saturated. From Fig. 7, we can see that a saturated sand flux relation can give a reasonable prediction on the windward side of the dune, far away from the dune's foot, where the depression of the wind occurs. In this region, however, the assumption of saturation cannot be employed (Wippermann and Gross, 1986; Weng et al., 1991; Sauermann et al., 2001). Hence, we need a model that allows for a nonsaturated sand flux and thus for saturation transients. In a previous study (Sauermann et al., 2001), we derived a continuum saltation model that can predict the sand flux on the entire windward side. In this model, the sand flux is defined in terms of a differential equation of the form

$$\frac{\partial}{\partial x} q = \frac{1}{l_s} q \left(1 - \frac{q}{q_s}\right), \tag{8}$$

where $q_s(u_*)$ is the saturated sand flux and $l_s(u_*)$ is the saturation length characterizing the dynamics of the saltation layer, i.e., a characteristic length for the saturation transients. The saturation length $l_s(u_*)$ depends on the shear velocity of the air, but converges towards a constant value for $u_* \gg u_{*t}$ (Sauermann et al., 2001). A typical solution of Eq. (8) is also shown in Fig. 7. The flux at the dune's foot is nonsaturated. It then increases monotonically from the dune's foot to the crest. This is not only a quantitative difference, but leads to a completely different prediction concerning the evolution of the dune's foot. In the saturated case, deposition would occur and the dune's foot would grow upwind (Wiggs et al., 1996), whereas in the nonsaturated case, erosion takes place and a downwind migration of the dune's foot is expected.

7. Dune migration

The spatial gradients of the sand flux $q(x)$ lead to erosion and thus to a temporal change in height of the sand bed. This can be expressed in terms of mass conservation as

$$\frac{\partial h}{\partial t} = -\frac{1}{\rho_{\text{sand}}} \frac{\partial q}{\partial x}, \tag{9}$$

where ρ_{sand} denotes the mean bulk density of the dune sand. This temporal change in height of the sand bed can be related to a horizontal surface velocity $v_s(x)$,

$$\frac{\partial h}{\partial t} = -v_s(x) \frac{\partial h}{\partial x}. \tag{10}$$

Here, we restrict ourselves to the case of a moving dune with invariant shape, where the surface velocity $v_s(x)$ becomes spatially constant, $v_s(x) = v_d = \text{constant}$. According to Eqs. (9) and (10), the dune velocity v_d is related to the change of flux with height,

$$v_d = \frac{1}{\rho_{\text{sand}}} \frac{dq}{dh}. \tag{11}$$

In Fig. 8, we show the dependence on height of measured and calculated sand fluxes according to Eqs. (6)–(8). At height zero, the saturated flux relations produce a vertical peak due to the decreasing flux in front of the dune's foot. For a dune that moves shape

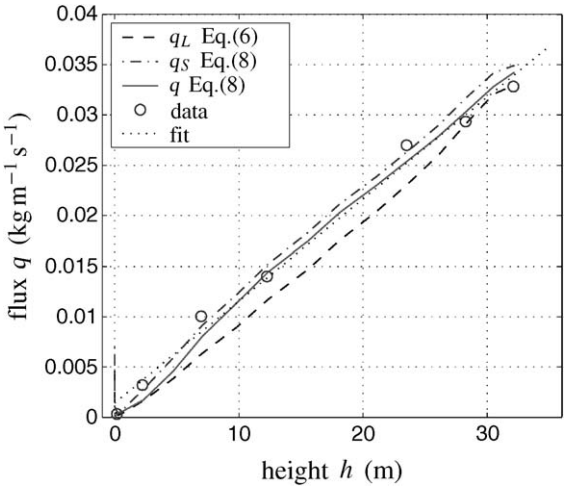

Fig. 8. The sand flux versus the height has to obey a linear relation for a dune that displaces with invariant shape in time. Accordingly, our study dune is an invariantly moving shape as the behavior of measured and calculated sand fluxes indicate. At the dune's foot, the validity of an equilibrium flux relation breaks down, which can be seen by the large increase of the flux at height zero.

invariantly ($v_s(x) = v_d$), a straight line with slope $v_d \rho_{sand}$ is expected. However, for a dune that is out of equilibrium ($v_s(x) \neq$ constant), any functional dependence can be obtained. Both the measured data and the calculated curves show a straight line. This suggests that the dune is in steady state and moves with invariant shape. Quantitatively, for the studied dune, we obtain a velocity v_d of 20 m year^{-1} using a shear velocity u_{*0} of 0.36 m s^{-1} and an average bulk density $\rho_{sand} = 1650$ kg m^{-3}. Both the shape invariance and the predicted dune velocity have been verified by comparing an aerial photograph from 1958 with the one shown in Fig. 3 from 1988.

8. Conclusion

In this study, we have shown through field measurements that a simplified analytical expression like Eq. (5) together with an heuristic approach to model the separation bubble can predict the shear stress of the air onto the windward side of a barchan dune. However, further work, based on general fluid dynamics equations, is still needed to confirm and improve this technique.

Our study also indicates that, apart from the region at the dune's foot, a saturated sand transport relation can provide reasonable predictions for the sand flux on the windward side of a dune. Calculations revealed that the relation proposed by Sørensen (1991) and our model reproduce the measured data better than the relation by Lettau and Lettau (1978). In addition, we have shown that a simple sand flux relation of the type $q(u_*)$ is not sufficient to model the sand flux at the dune's foot, where the assumption of saturation breaks down. It is then suggested and confirmed by numerical simulation that this problem can be naturally solved by a continuum saltation model that allows for out-of-equilibrium conditions. Finally, from a simple analysis of the dynamical behavior of the measured dune, we conclude that it moves with invariant shape.

Summarizing, our field measurements confirm the validity of our equations of motion and in particular underline the importance to take into account the transient effects of the sand flux towards saturated values. With these existing equations, it is now possible to understand better the shape evolution and the movement of different types of dunes. Another future application of our equations should be the simulations of techniques to control sand motion.

Acknowledgements

We acknowledge the support of this work by the Deutsche Forschungsgemeinschaft (DFG) under contract no. HE 2732/1-1. We also acknowledge the Brazilian agencies CNPq, CAPES and FUNCAP for financial support.

References

Bagnold, R.A., 1936. The movement of desert sand. Proc. R. Soc. Lond., A 157, 594–620.

Bagnold, R.A., 1941. The Physics of Blown Sand and Desert Dunes. Methuen, London.

Butterfield, G.R., 1993. Sand transport response to fluctuating wind velocity. In: Clifford, N.J., French, J.R., Hardisty, J. (Eds.), Turbulence: Perspectives on Flow and Sediment Transport. Wiley, Chichester, pp. 305–335.

Carruthers, D.J., Hunt, J.C.R., 1990. Fluid mechanics of airflow over hills: turbulence, fluxes, and waves in the boundary layer. In: Blumen, W. (Ed.), Atmospheric Processes over Complex Terrain, vol. 23. Am. Meteorol. Soc., Boston, pp. 83–108.

Hastenrath, S., Greischar, A., 1993. Circulation mechanisms related to Northeast Brazil rainfall anomalies. J. Geophys. Res. 98, 5093–5102.

Hunt, J.R.C., Leibovich, S., Richards, K.J., 1988. Turbulent wind flow over smooth hills. Q. J. R. Meteorol. Soc. 114, 1435–1470.

Jackson, P.S, Hunt, J.C.R., 1975. Turbulent wind flow over a low hill. Q. J. R. Meteorol. Soc. 101, 929.

Jimenez, J.A., Maia, L.P., Serra, J., Morais, J., 1999. Aeolian dune migration along the Ceará coast, north-eastern Brazil. Sedimentology 46, 689–701.

Kroy, K., Sauermann, G., Herrmann, H.J., 2002. A minimal model for sand dunes. Phys. Rev. Lett. 88, 54301.

Lancaster, N., 1995. Geomorphology of Desert Dunes. Routledge, London.

Lancaster, N., Nickling, W.G., McKenna Neumann, C.K., Wyatt, V.E., 1996. Sediment flux and airflow on the stoss slope of a barchan dune. Geomorphology 17, 55–62.

Lettau, K., Lettau, H., 1978. Experimental and micrometeorological field studies of dune migration. In: Lettau, H.H., Lettau, K. (Eds.), Exploring the World's Driest Climate. Center for Climatic Research Univ. Madison, Wisconsin.

Maia, L.P., 1998. Procesos Costeros y Balance Sedimentario a lo Largo de Fortaleza (NE Brazil): Implicationes para una Gestión Adecuada de la Zona litoral. PhD thesis, Faculty of Geology, University of Barcelona.

Markham, C.G., McLain, D.R., 1977. Sea surface temperature related to rain in Ceará, north-eastern Brazil. Nature 265, 320–323.

Nobre, P., Shukla, J., 1996. Variations of sea surface temperature, wind stress, and rainfall over the Tropical Atlantic and South America. J. Climate 9, 2464–2479.

Philander, S.G.H., Pacanowski, R.C., 1986. A model of the seasonal cycle in the tropical Atlantic Ocean. J. Geophys. Res. 91, 14192–14206.

Pye, K., Tsoar, H., 1990. Aeolian Sand and Sand Dunes. Unwin Hyman, London.

Sauermann, G., Kroy, K., Herrmann, H.J., 2001. A continuum saltation model for sand dunes. Phys. Rev. E 64, 31305.

Sørensen, M., 1991. An analytic model of wind-blown sand transport. Acta Mech., Suppl. 1, 67–81.

van Dijk, P.M., Arens, S.M., van Boxel, J.H., 1999. Aeolian processes across transverse dunes: II. Modelling the sediment transport and profile development, 1999. Earth Surf. Process. Landf. 24, 319–333.

Weng, W.S., Hunt, J.C.R., Carruthers, D.J., Warren, A., Wiggs, G.F.S., Livingstone, I., Castro, I., 1991. Air flow and sand transport over sand-dunes. Acta Mech., Suppl. 2, 1–22.

White, B.R., Mounla, H., 1991. An experimental study of Froud number effect on wind-tunnel saltation. Acta Mech., Suppl. 1, 145–157.

Wiggs, G.F.S., Livingstone, I., Warren, A., 1996. The role of streamline curvature in sand dune dynamics: evidence from field and wind tunnel measurements. Geomorphology 17, 29–46.

Wippermann, F.K., Gross, G., 1986. The wind-induced shaping and migration of an isolated dune: a numerical experiment. Bound. Layer Meteorol. 36, 319–334.

Zeman, O., Jensen, N.O., 1988. Progress Report on Modeling Permanent Form Sand Dunes. Risø National Laboratory, M-2738.